JOURNAL OF MOLECULAR SPECTROSCOPY **101**, 358–368 (1983)

The Electronic Valence States of CuO: Radiative Lifetimes of the *A*, *A'*, *C*, and *D* States

J. M. DELAVAL, F. DAVID, Y. LEFEBVRE, P. BERNAGE, P. NIAY, AND J. SCHAMPS

Laboratoire de Spectroscopie des Molécules Diatomiques, Equipe de Recherche associée au CNRS n° 303, Bâtiment P5, Université des Sciences et Techniques de Lille I, 59655 Villeneuve d'Ascq Cédex, France

Radiative lifetimes of several electronic states of CuO have been determined by recording the exponential decay of the fluorescence following resonant excitation by a pulsed dye laser. The lifetimes extrapolated to zero pressure have been found to be 0.65 μsec for the $A^2\Sigma^-$ state, 1.3 μsec for the $C^2\Pi$ state, 1.8 μsec for the $D^2\Delta$ state, and more than 5 μsec for the A' ($\Omega = 1/2$) state. In connection with an energy level diagram, these values support the assignment of the *A*, *C*, and *D* states, to the $3d^9_{Cu^+}\ 4s_{Cu^+}\ 2p^5_{O^-}$ ($\sigma^2\ \pi^3$) structure. The long-lived A' state could be either another doublet or a contaminated quartet $\Omega = 1/2$ component of the same structure as the three other states or a state of the $3d^9_{Cu^+}\ \sigma^{*2}\ 2p\pi^4$ structure.

I. INTRODUCTION

The electronic spectrum of the CuO molecule has been extensively investigated during the past 20 years (*1–7*). After a period of confusion, probably due to the unusual aspect of many of the bands, the first correct vibrational and rotational analysis of CuO bands dates back to 1973 (*2*). Today, bands belonging to no less than 15 different electronic transitions lying in the visible and near infrared spectral regions have been observed; all of them are connected with the $X^2\Pi_i$ ground state. In view of the features of these bands, symmetry assignments (Λ, *S*, Ω) have been suggested for the observed states. Except for the $k^4\Sigma^-$ state (*4*) they are all considered to be doublet states. In fact, up to now, little progress has been made to clarify the electronic configurations of these states. For only two states, namely the $X^2\Pi_i$ ground state and the recently observed $Y^2\Sigma^+$ state, have the configurations been identified unambiguously; these states are, respectively, the $\sigma^2\ \pi^3$ and the $\sigma\ \pi^4$ components of the Cu^+ ($3d^{10}$) O^- ($2p^5$) structure (*7*). Nothing is clear about the configurations of the other states of CuO; some of them could even be assumed to be components of quartet states being able to radiate towards $X^2\Pi$ owing to strong spin–orbit contamination by doublet states. Rigorously speaking and in relation with rotational analysis, the only electronic quantum number unambigously defined for these states is the value of Ω, the projection of the total angular momentum on the internuclear axis.

New information is needed to go further towards an identification of the electronic configurations of these excited states. In the preceding paper some of us (Y.L. and J.S.) used ab initio calculations to construct an energy-level diagram of the lowest-lying valence states of CuO. The present paper is intended to provide experimental results about the radiative lifetimes of four of the observed electronic states, namely,

0022-2852/83 $3.00

the A' ($\Omega = 1/2$), $A^2\Sigma^-$ ($\Omega = 1/2$), $C^2\Pi$ ($\Omega = 1/2, 3/2$), and $D^2\Delta$ ($\Omega = 3/2, 5/2$) states lying at term values T_e equal to 15 862, 16 809, 19 209, and 19 473 cm^{-1}, respectively. This experimental study coupled with the ab initio one reported in the preceding paper enables us to suggest electronic configurations for the four states.

II. EXPERIMENTAL DETAILS

The apparatus used to determine radiative lifetimes of the CuO excited electronic states is described here. The optical excitation pulses were provided by a Hänsch design grating-tuned dye laser pumped by a Jobin-Yvon LA 04S nitrogen laser (20-Hz repetition rate, 7-nsec pulse duration, 3.5-mJ/pulse energy). Several dyes were selected according to the spectral range of the pumped transitions: rhodamine 600 for the A–X system, coumarin 540 for the C–X and D–X systems, rhodamine 640 for the A'–X system. Typical characteristics for the dye laser pulse were 6-nsec duration, 0.2-mJ/pulse energy, and 0.4-cm^{-1} FWHM linewidth.

Gas phase CuO was generated using the reaction of copper vapor with N_2O in a Broida-type flow system (*8*) pumped by a double stage 600 liter/min mechanical pump. The metal atoms in the flow reactor were evaporated from an open stainless steel crucible and carried up either in a N_2O or an argon flow monitored by gate valves. BK7 windows of the reaction chamber allowed laser beam entry and photomultiplier detection at right angle to the laser beam. During the experiments the pressure in the pumped chamber was fixed in the range 0.005–1 Torr as measured with a capacitor-type pressure transducer.

During lifetime measurements, the dye laser was tuned to a wavelength that lies within an electronic absorption band system of CuO. Wavelength selection of the fluorescence emission was achieved by means of a Jobin-Yvon HRS monochromator equipped with a 1200 grooves mm^{-1} grating blazed at 0.5 μm. The fluorescence was then detected by using a R 928 Hamamatsu photomultiplier (rise time: 3 nsec). The photomultiplier signal was amplified through a bandpass amplifier 100 Hz–100 MHz and then sent to a 256-gate transient numerical averager (time resolution: 10 ns). Typically, signals from 10^3 to 10^4 laser pulses were accumulated for each experiment. Possible systematic errors, due, for instance, to residual scattered light or to slight defects in the detection system, were minimized by using a process of difference between the signal obtained with oxidizer on and the one obtained with oxidizer off, replaced by argon at the same pressure.

The data were analyzed using Provencher's computer program (*9*), especially designed for extracting exponential decay function from a signal plus random noise, with an unknown constant baseline.

III. LIFETIMES

(A) Preliminary Remarks

In our experiments we observe the exponential decay of the fluorescence light following resonant excitation by a pulsed dye laser. In the case where the results can be described by a single state model and if the pressure is not too high, the total depopulation rate of a molecular excited state is essentially due to radiative and quenching processes:

$$N_m = N_m^0 e^{-\gamma t}$$

where, at fixed temperature, $\gamma = (1/\tau) + Q$ depends on pressure following the Stern-Volmer law (*10*) (N_m: population density of state m; τ: radiative lifetime; Q: quenching probability).

On the other hand, we observe in some cases more complicated exponential decay. If the excited molecular state m is populated from other states k via a quenching process the situation is described by

$$\frac{dN_m}{dt} = -\frac{N_m}{\tau_m} + \sum_k W_{km} N_k$$

Solutions are multiple-exponential decay functions the time constants of which can be calculated from the individual lifetimes but should not be confused with them (*9*).

(B) Results

The energy level diagram of the A', A, C, and D states of the CuO molecule is shown in Fig. 1.

The experimental purpose was to obtain a selectively detected fluorescence excitation spectrum from laser radiation tuned to a narrow wavelength range covering the bandhead region. In all cases, to eliminate the influence of scattered laser light, observation of the fluorescence signal was done by setting the monochromator (spectral bandwidth 10 cm^{-1}) on a band well separated from the one excited by the laser. Depending on the selection rules relevant to the various observed transitions, this means that observation was made via another spin–orbit subsystem as explained later. The wavelength regions analyzed in the different experiments are indicated in Table I. They correspond to maximum fluorescence signal intensity. Nevertheless, except for the C–X transition, the observed fluorescence emission cannot be ascribed to a single vibrational state because of the fairly large spectral width of the exciting radiation (0.4 cm^{-1}) which covers not only the head studied but also lines of other close-lying bands of the same frequency.

The $A^2\Sigma^-$ State

The pump laser was tuned to the $A^2\Sigma^- - X^2\Pi_{3/2}$ 0–0 bandhead (6059 Å) and the fluorescence was observed from the $A^2\Sigma^- - X^2\Pi_{1/2}$ 0–0 band (6160 Å). Thus, even though the monochromator bandwidth was fairly large (10 cm^{-1}) scattered laser light did not perceptibly interfere with lifetime measurements. A $A^2\Sigma^- - X^2\Pi_{1/2}$ fluorescence decay curve is shown in Fig. 2 as an example for a specific condition of total pressure (0.2 Torr). The signal-to-noise ratio (30:1) averaging over 2048 shots is typical of the experiments performed at pressures around 0.1–1 Torr. However, at lower pressure, the signal-to-noise ratio decreases. At all pressures below 5 Torr, the fluorescence decay curve is well represented by a single exponential decay constant. The corresponding Stern–Volmer diagram is shown in Fig. 3. From this diagram, the radiative

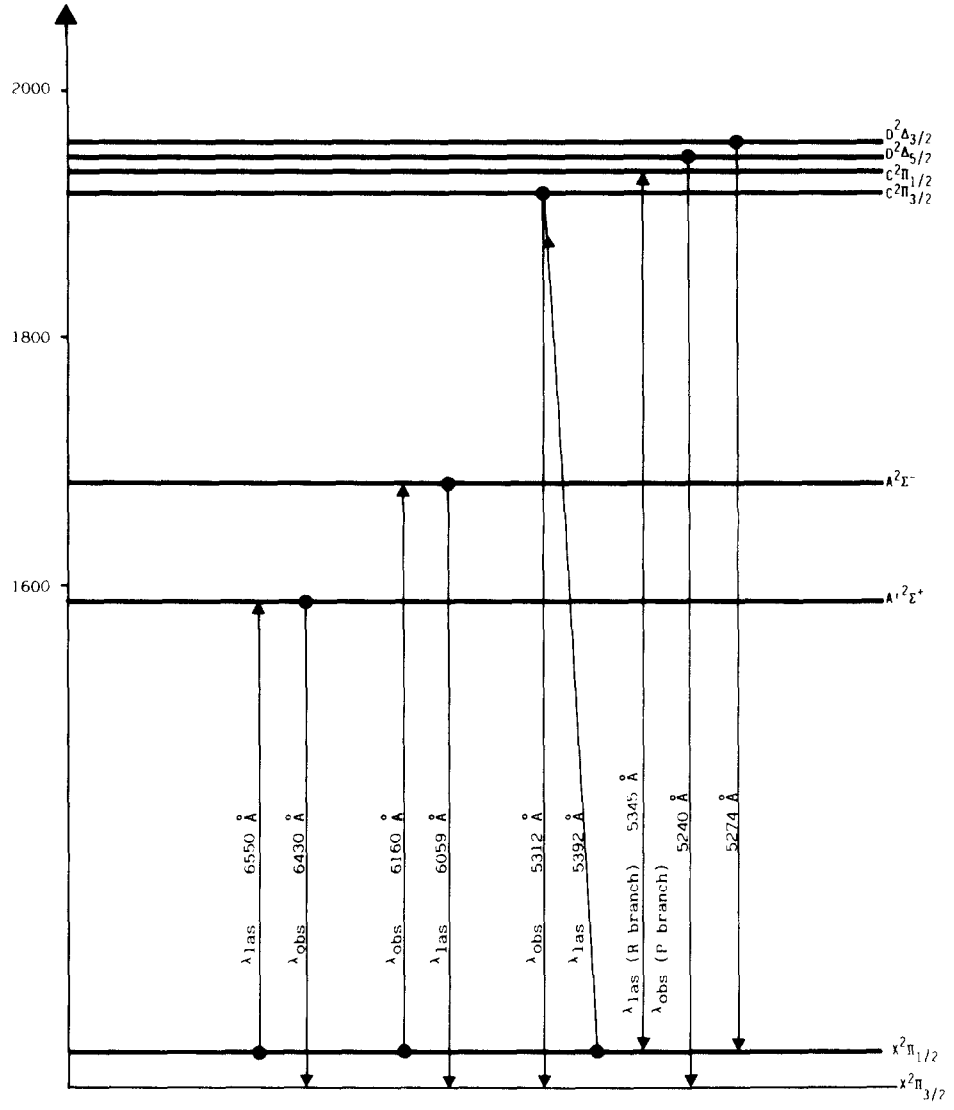

FIG. 1. Electronic levels of CuO involved in the lifetime experiments. λ_{las} indicated where the laser was tuned; λ_{obs} indicated observation of fluorescence signals was achieved by tuning the monochromator.

lifetime of the $A^2\Sigma^-$ state, obtained by extrapolating the measured τ to zero pressure,[1] was found to be 0.65 ± 0.04 μsec.

[1] The resonance fluorescence can be trapped by multiple scattering of resonance photons if the density of absorbing molecules is sufficient to induce significant self-absorption; this effect is known as radiation trapping. When this phenomenon is observed, the apparent radiative lifetime obtained by extrapolation to zero pressure is larger than the true one. Thorough treatments of this problem have been given by Holstein (*11*) and Holt (*12*). In the present experiments, however, the partial pressure of CuO gas in the vapor was roughly estimated to be 10^{11} molecules cm^{-3}, although difficult to confidently specify (*13*), so that effect of radiation trapping should be smaller than the experimental uncertainty of the lifetime measurement.

TABLE I

Measured Radiative Lifetimes of CuO Lower States

Electronic state	Excitation wavelength (Å)	Observation wavelength	v' - v''[a] band	Lifetime μs	Statistical uncertainty μs
$A^2\Sigma^-$	6059	6160	0 - 0	0.65	0.04
$A'^2\Sigma^+$	6550	6430	0 - 0	> 5	0.5
$C^2\Pi$	5312	5392	0 - 0	1.30	0.09
$D^2\Delta$	5412	5240	0 - 0	1.80	0.16

[a] These v' - v'' values are only approximate since bands of the source sequence are overlapped.

The $A'^2\Sigma^+$ State

The lifetime measurements for the A' state involved poor signal-to-noise ($S/N \simeq 4$) averaging over 8192 shots, even under the most optimized experimental conditions. This results in poor accuracy in the measurements, and uncertainties up

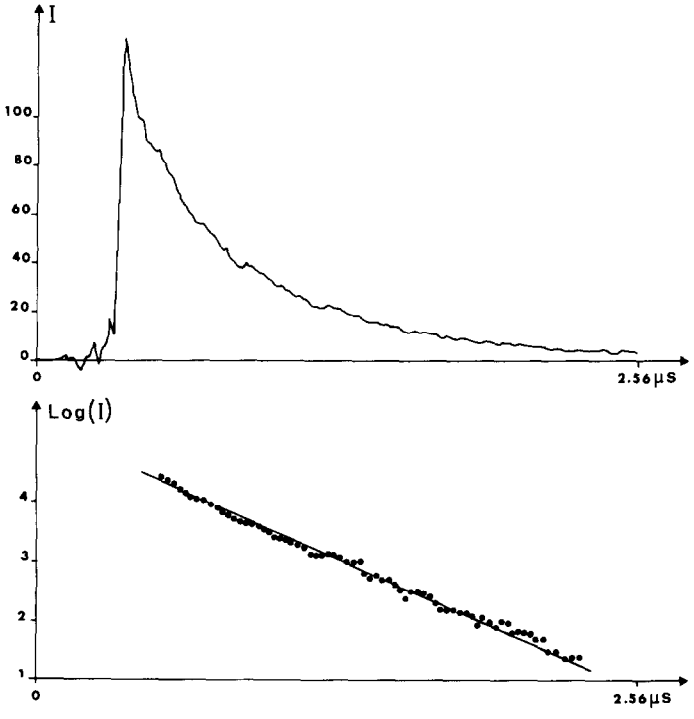

FIG. 2. Typical fluorescence decay curve (A state; pressure: 0.2 Torr).

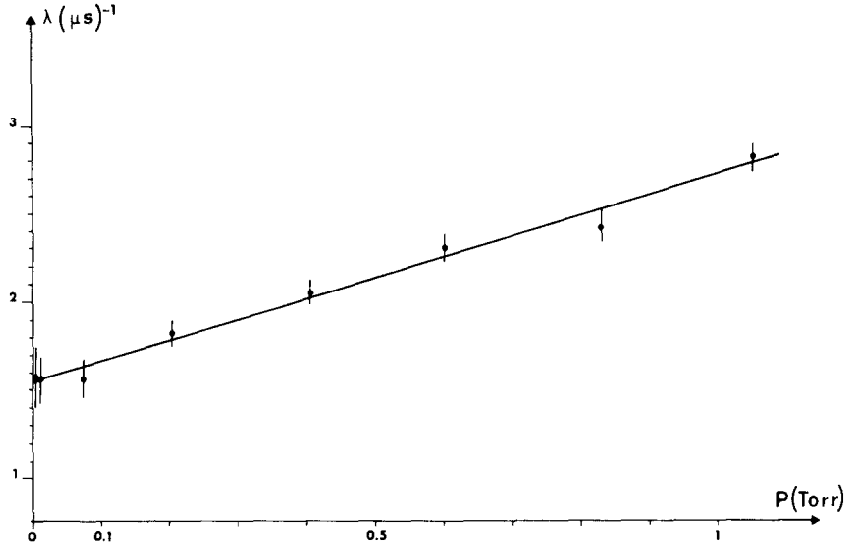

FIG. 3. Stern-Volmer diagram (A state).

to 20% were the rule. At any rate, our measurements indicate that the radiative lifetime of the A' state is longer than 5 μsec. Another method was also used to populate the A' state. It consisted in pumping into the easier-to-populate A state, the A' state being populated from the A state through $A \rightarrow A'$ collisional transfer. The measurements obtained by this method did not really improve the A' state lifetime accuracy but they confirmed that the A' state is longer lived than the A state.

The $C^2\Pi$ and $D^2\Delta$ States

These two states yield emissions to the $X^2\Pi$ ground state observed in the green region of the spectrum (see Fig. 1). It is convenient to discuss them simultaneously because recent spectroscopic studies (*5*) have shown that they are affected by spin–orbit perturbation. This interaction is not perceptible when looking at $\Delta\Sigma = 0$ transitions which can be fairly well described by using a typical case (a) model. Rather, the interaction is revealed by the occurrence of "forbidden" $|\Delta\Sigma| = 1$ intercombination bands besides the $\Delta\Sigma = 0$ bands normally expected in pure case (a). One of these intercombination bands, namely the $C^2\Pi_{3/2}$–$X^2\Pi_{1/2}$ transition, is as intense as the $\Delta\Sigma = 0$ bands.

This special feature allowed the lifetime of the $C^2\Pi_{3/2}$ component to be studied in exactly the same way as for the A and A' states (see Fig. 1 and Table I). The radiative lifetime of the $C^2\Pi$ state measured in its $v = 0$ level and extrapolated to zero pressure was found to be 1.3 ± 0.1 μsec.

Lifetime measurements were also carried out on the fairly intense $\Delta v = -1$ sequence of the $C^2\Pi_{3/2}$–$X^2\Pi_{3/2}$ system. In this sequence, the bandheads are well separated (7 Å) and the intensity is more equally distributed between the bands than in the principal $\Delta v = 0$ sequence so that the three first bands of the $\Delta v = -1$ sequence could be studied separately. Within experimental errors, no lifetime dependence on the vi-

brational quantum number was found, which probably means that the transition moments vary slowly with the internuclear separation.

Due to the lack of a sufficiently intense intercombination band, lifetime measurements on the $C^2\Pi_{1/2}$–$X^2\Pi_{1/2}$ system were performed by pumping the R head of the 0–0 band (λ = 5345 Å) and recording the resulting fluorescence from the P branch (see Fig. 1 and Table I). In this case, the spectral proximity between the laser excitation line and the observed fluorescence made detection more difficult and the signal-to-noise ratio worse and in the $C^2\Pi_{3/2}$ study because the spectral bandwidth of the monochromator had to be reduced. Within experimental uncertainty ($\simeq$0.1 μsec), the $C^2\Pi_{1/2}$ lifetime was found equal to the $C^2\Pi_{3/2}$ lifetime, i.e., 1.3 μsec.

The same method, i.e., pumping in the R(0–0) band, detection in the P(0–0), could have been used for the lifetime measurements of the $D^2\Delta$ state which also shows only weak intercombination bands with the ground state. However, in this case, it appeared more efficient to use a different method. The laser line was tuned onto bands of the $\Delta v = -1$ sequences of the $D^2\Delta_{5/2}$–$X^2\Pi_{3/2}$ (λ = 5420 Å) and $D^2\Delta_{3/2}$–$X^2\Pi_{1/2}$ (λ = 5453 Å) transitions and detection was carried out in the corresponding $\Delta v = 0$ sequences (λ = 5240 5274 Å, respectively). For both spin–orbit components, the lifetime of the $D^2\Delta$ state was found to be 1.8 $\pm$ 0.2 μsec.

(C) Cascading Processes

We have qualitatively investigated the dynamical behavior of the different excited states under collisional conditions. Eventual cascading processes are expected to increase the measured lifetime (*14*). Their presence is revealed through two kinds of phenomena when an inert quenching gas (argon) is introduced: first, when the laser beam is absorbed through a resonance transition, other fluorescence electronic transitions appear besides the fluorescence signal from the resonance transition; second, on the resonance fluorescence decay curves a "tail" can be observed, the amplitude of which grows as the pressure increases.

An example of the first kind of phenomena was found for the $A^2\Sigma^-$ state. The laser wavelength was set on either one of the $A^2\Sigma^-$–$X^2\Pi$ components and fluorescence decays of the two $A'\ ^2\Sigma^+$–$X^2\Pi$ transitions were observed. Then, following A state optical pumping, there appears a collisional $A \rightarrow A'$ transfer followed by A'–X decay. As mentioned previously, the long lifetime measured by this method for the A' state corroborates the results of the experiments using direct pumping. $A \rightarrow \beta$ transfers, weaker than $A \rightarrow A'$ ones, were also observed by pumping in the A state at 1 Torr argon pressure. No radiative lifetime could be deduced for the β state because of the weakness of the signal for other pressures. In the same way, when one pumped the C–X transition, A–X fluorescence decay was observed (Fig. 4) with a delay corresponding to $C \rightarrow A$ transfer. We also observed transfers from the C state to the D state which is situated slightly (550 cm^{-1}) higher in energy (Fig. 1).

To illustrate the second kind of phenomena due to cascading, let us consider the fluorescence decay of the A state at different pressures of argon ranging from 5 to 20 Torr. As argon pressure is increased, the lifetime is reduced and the fluorescence decay of the A state acquires a more and more prominent tail (Fig. 5). Inspection of this double-exponential decay behavior shows that this tail corresponds to a lifetime in agreement with that of the A' state.

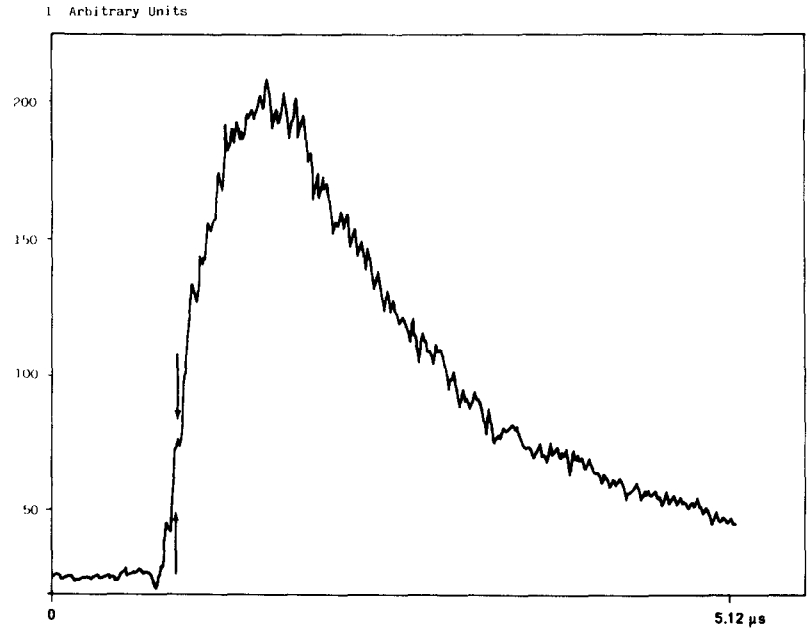

FIG. 4. Fluorescence branching C–A–X decay curve. Fluorescence of the $A^2\Sigma^-$ state (τ_A = 0.65 μsec) appears with a delay corresponding to C–A transfer (τ_C = 1.30 μsec). The arrow indicates the laser pulse. λ_{laser}:5312 Å, λ_{obs}:6060 Å.

It is worthwhile to notice that cascading processes that invalidate lifetime measurements may also have positive applications. Thus, collisional transfer was used by several authors (*6, 7*) to discover some low-lying valence states of CuO by populating them via the A state.

IV. DISCUSSION

The ab initio energy level diagram in the preceding paper constitutes the basis for interpreting the magnitude of the radiative lifetimes determined in the present work. Since the $X^2\Pi$ ground state and the first excited state $Y^2\Sigma^+$ have already been identified as the two components of the $3d^{10}_{Cu^+}\ 2p^5_{O^-}$ structure (*7*), it follows from the energy level diagram of the preceding paper that all the other observed states of CuO, among which are the four states considered here, should belong to either one of the two low-lying structures corresponding to an unfilled $3d$ shell, namely the structures designated as Structures III and IV in the preceding paper. Table II summarizes all states belonging to these structures. It is noteworthy to point out that in the region of equilibrium internuclear separations, all the molecular orbitals have been found from our ab initio calculations to be fairly localized on one of the two atoms, Cu^+ or O^-, except for the so-called σ^* orbital of Structure III that forms a bond between the $4s_{Cu^+}$ and $2p\sigma_{O^-}$ orbitals.

Perhaps the most remarkable result of the experiments reported above is that all the lifetimes measured in CuO are quite long, even that of the $A^2\Sigma^-$ state that is known to give the strongest bands of the molecule. This can be understood by noticing

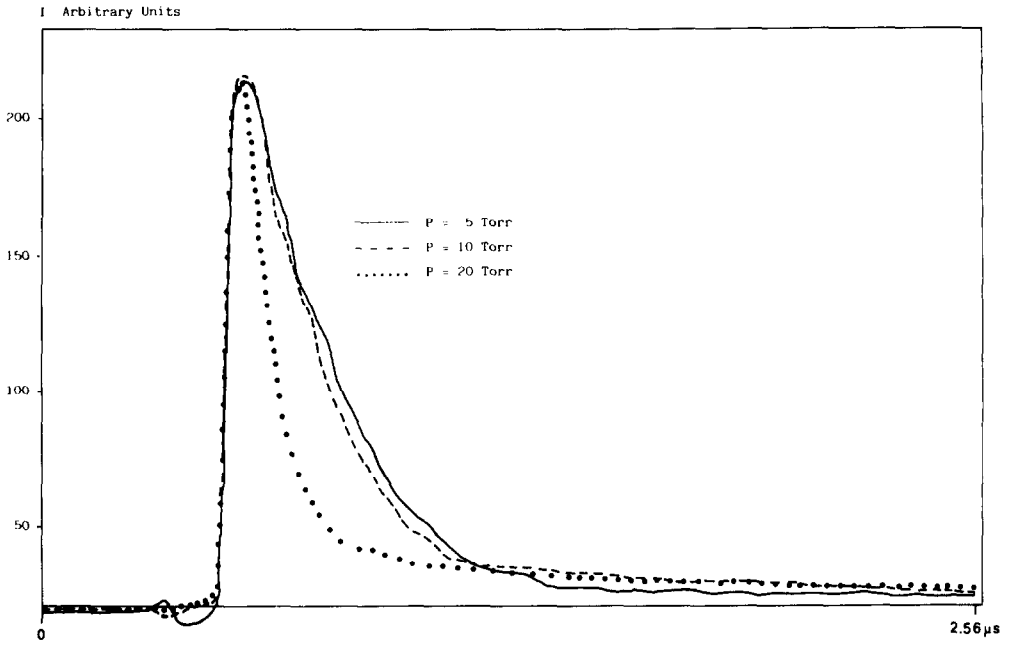

FIG. 5. Fluorescence signals from the $A^2\Sigma^-$ state of CuO illustrating the effect of a quenching gas (argon) on the shape of the fluorescence decay curve.

that Structures III and IV differ from the two low-lying states $X^2\Pi$ and $Y^2\Sigma^+$ by at least a $3d$–$4s$ replacement. This is a forbidden electronic transition in the atomic limit and for that matter, the corresponding $(3d^9\ 4s)^2D$–$(3d^{10})^2S$ transition lines in

TABLE II

Electronic States and Corresponding Spin–Orbit Components for the Two Cu^+ ($3d^9$) Low-lying Structures of CuO

Structure	3d-hole	Electronic states	Spin-orbit components (Ω)*
III : $3d^9_{Cu^+}\ \sigma^{*2}\ 2p\pi^4_{O^-}$	3dδ	$^2\Delta$	3/2 , 5/2
	3dπ	$^2\Pi$	1/2 , 3/3
	3dσ	$^2\Sigma^+$	1/2
IV : $3d^9_{Cu^+}\ 4s_{Cu^+}\ 2p^5_{O^-}(\sigma^2\pi^3)$	3dδ	$^4\Phi$, $^2\Phi(2)$, $^4\Pi$, $^2\Pi(2)$	9/2, 7/2(3), 5/2(4), 3/2(4), 1/2(3), -1/2
	3dπ	$^4\Delta$, $^2\Delta(2)$, $^4\Sigma^+$, $^2\Sigma^+(2)$, $^4\Sigma^-$, $^2\Sigma^-(2)$	7/2, 5/2(3), 3/2(5), 1/2(7)
	3dσ	$^4\Pi$, $^2\Pi(2)$	5/2, 3/2(3), 1/2(3), -1/2

* Numbers in parentheses give the number of components corresponding to the Ω value they follow.

Cu^+, although they connect the two lowest-lying states of the ion, are not included in standard wavelength tables as complete as MIT's (*15*). That $3d$–$4s$ transitions appear in the CuO molecule can be explained by s and p polarization of the $3d\sigma$ and $3d\pi$ orbitals. However, in no way can one expect from them transition probabilities as large as for fully electronically allowed transitions.

Let us now try to identify more precisely the nature of each of the four states considered in these experiments. As stated above, the A state is the excited state that yields the most intense transition into $X^2\Pi$ in the CuO spectrum. It is also the one that has the shortest lifetime ($\tau = 0.65$ μsec) of all the states of CuO for which this property is known. From this we conclude that the A–X transition must be a spin-allowed transition so that the A state is a doublet state. Previous rotational analysis (*2*) has proved that the electronic parity of the A state is opposite to that of the Y state which has been established to be a $^2\Sigma^+$ state (*7*). Therefore, the A state must be a $^2\Sigma^-$ state. There are only two $^2\Sigma^-$ states in the energy level diagram. They both belong to the same configuration, namely,

$$3d^9_{Cu^+}\,(\sigma^2\,\pi^3\,\delta^4)\,4s_{Cu^+}\,2p^5_{O^-}\,(\sigma^2\,\pi^3).$$

It is most likely that the $A^2\Sigma^-$ state is one of these two states. We notice that its experimental term value ($T_e = 16\,809$ cm^{-1}) coincides fairly well with the calculated term value of the lowest of these two states ($T_e = 16\,000$ cm^{-1}). But the accuracy of the energy level diagram is not sufficient to use this argument as a proof that the $A^2\Sigma^-$ state is undoubtedly the lowest $^2\Sigma^-$ state of CuO.

The lifetimes of the C and D states are, respectively, twice and three times that of the $A^2\Sigma^-$ state. This same order of magnitude leads us to think that they belong to the same structure as the A state (Structure IV) and that they are also predominantly doublet states. Therefore, we suggest for them the following configurations:

$$3d^9_{Cu^+}\,(\sigma\,\pi^4\,\delta^4)\,4s_{Cu^+}\,2p^5_{O^-}\,(\sigma^2\,\pi^3) \qquad \text{for} \qquad C^2\Pi$$

$$3d^9_{Cu^+}\,(\sigma^2\,\pi^3\,\delta^4)\,4s_{Cu^+}\,2p^5_{O^-}\,(\sigma^2\,\pi^3) \qquad \text{for} \qquad D^2\Delta$$

(the latter configuration is the same as that of the $A^2\Sigma^-$ state). Given that the first of these configurations lies, on the average, lower than the second one, it is likely that the $D^2\Delta$ state is the lowest of the two $^2\Delta$ states of its configuration whereas the $C^2\Pi$ state is the highest of the two $^2\Pi$ states of its configuration. In this model, the strong coupling between the $C^2\Pi$ and $D^2\Delta$ states, experimentally revealed by the occurrence of intercombination bands (5), is a consequence of the pure precession spin–orbit interaction between the $3d\sigma$ and $3d\pi$ orbitals by which the two configurations differ.

The last state, A', has a markedly longer lifetime than the three others. There are several possibilities for its configuration. First, it could belong to the same structure as the A, C, and D states. It would then be either a long-lived $^2\Sigma^+$ state or, more likely, one of the quartet states of Structure IV that some spin–orbit interaction with a close-lying doublet state of the same structure would make it capable of radiating to the ground state. Such a case of contamination leading to a lifetime of similar magnitude (7 μsec) has been found (*15*) for a comparable ($3d^9\ 4s$) state ($a^3\Pi$) of another copper compound, CuF (*16*). Another hypothesis would be to assign the A' state to Structure III. In this case, its $3d^9_{Cu^+}\,(4s_{Cu^+} + 2p\sigma_{O^-})^2\,2p\pi^4_{O^-}$ structure would

differ from the $3d^{10}_{Cu^+}\ 2p^5_{O^-}$ ($\sigma^2\ \pi^3$) configuration of the $X^2\Pi$ state by a double electronic excitation and from that of the $3d^{10}_{Cu^+}\ 2p^5_{O^-}$ ($\sigma\ \pi^4$) configuration of the $Y^2\Sigma^+$ state by a single electronic excitation. But these excitations would have to be accompanied by a rearrangement of the bonding σ^* orbital into a nonbonding orbital and this would be the reason for the anomalously long lifetime of the A' state.

RECEIVED: April 12, 1983

REFERENCES

1. A. LANGERQVIST AND U. UHLER, *Z. Naturforsch.* **226,** 551 (1967).
2. O. APPELBLAD AND A. LAGERQVIST, *Phys. Scr.* **10,** 307–324 (1973).
3. Y. LEFEBVRE, B. PINCHEMEL, AND J. SCHAMPS, *J. Mol. Spectrosc.* **68,** 81–88 (1977).
4. O. APPELBLAD, A. LAGERQVIST, AND M. LYYRA, *Phys. Scr.* **18,** 137–140 (1978).
5. O. APPELBLAD, A. LAGERQVIST, Y. LEFEBVRE, B. PINCHEMEL, AND J. SCHAMPS, *Phys. Scr.* **18,** 125–136 (1978).
6. O. APPELBLAD, A. LAGERQVIST, J. RENHORN, AND R. W. FIELD, *Phys. Scr.* **22,** 603–608 (1981).
7. Y. LEFEBVRE, B. PINCHEMEL, J. M. DELAVAL, AND J. SCHAMPS, *Phys. Scr.* **25,** 329–332 (1982).
8. J. B. WEST, R. S. BRADFORD, JR., J. D. EVERSOLE, AND C. R. JONES, *Rev. Sci. Instrum.* **46,** 164–168 (1975).
9. S. W. PROVENCHER, *J. Chem. Phys.* **64**(7), 2772–2777 (1976).
10. O. STERN AND M. VOLMER, *Z. Phys.* **20,** 183–194 (1910).
11. T. HOLSTEIN, *Phys. Rev.* **72,** 1212–1226 (1947).
12. H. K. HOLT, *Phys. Rev. A* **13**(4), 1442–1447 (1976).
13. F. SMYTH AND S. ROBERTS, *J. Amer. Chem. Soc.* **43,** 1061–1067 (1928).
14. C. R. QUICQ, JR., AND R. E. WESTON, *J. Chem. Phys.* **74,** 4951–4959 (1974).
15. R. E. STEELE AND H. P. BROIDA, *J. Chem. Phys.* **69,** 2300–2305 (1978).
16. C. DUFOUR, J. SCHAMPS, AND R. F. BARROW, *J. Phys. B* **15,** 3819–3828 (1982).